Available online at www.sciencedirect.com
ScienceDirect
Journal of Environmental Sciences 2010, 22(4) 507–511
JOURNAL OF ENVIRONMENTAL SCIENCES
ISSN 1001-0742
CN 11-2629/X
www.jesc.ac.cn

Adsorption behavior of phosphate on Lanthanum(III) doped mesoporous silicates material

Jianda Zhang[1], Zhemin Shen[1,*], Wenpo Shan[2], Ziyan Chen[3], Zhijian Mei[1], Yangming Lei[1], Wenhua Wang[1]

1. School of Environmental Science and Engineering, Shanghai Jiaotong University, Shanghai 200240, China. E-mail: zjdrf@163.com
2. College of Chemistry and Environmental Science, Hebei University, Baoding 071002, China
3. College of Life and Environmental Sciences, Shanghai Normal University, Shanghai 200234, China

Received 11 June 2009; revised 12 November 2009; accepted 16 November 2009

Abstract

A series of lanthanum doped meosoporous MCM-41 (La_xM41, *x* is Si/La molar ratio) was prepared by sol-gel method. The surface structure of the materials was investigated with X-ray diffraction and N_2 adsorption/desorption technique. The content of La in the materials was determined by ICP. It was found that the La content of La_{25}M41, La_{50}M41 and La_{100}M41 was 7.53%, 3.89% and 2.32%, respectively. The phosphate adsorption capacities increased with increasing amount of La incorporation. With 0.40 g La_{25}M41 99.7% phosphate could be removed. The effects of Si/La molar ratio, La_xM41 dose, pH, initial concentration of phosphate solution, co-ions on phosphate adsorption were also evaluated. The phosphate adsorption kinetics of La_xM41 could be well-described by the pseudo second-order model, and Langmuir isotherm fit equilibrium data much better than the Freundlich isotherm.

Key words: lanthanum doped; mesoporous material; phosphate adsorption; eutrophication

DOI: 10.1016/S1001-0742(09)60141-8

Introduction

Phosphorus is the key nutrients for biological and chemical processes in natural water bodies, and large quantity of phosphate present in wastewater is one of the main causes of eutrophication in surface waters (Chubar et al., 2005; Saad et al., 2007). Therefore, strict discharge standards of phosphate (0.5–1.0 mg P/L) were applied to control the level of phosphate in water (Ugurlu and Salman, 1998). Physicochemical and biological techniques have been used for phosphate removal. Among these methods, adsorption technique is effective and economical, however, the key problem is how to find efficient, low-cost and easily available adsorbents. Many inorganic adsorption materials, such as alum and aluminum hydroxide (Georgantas and Grigoropoulou, 2007), zeolite (Onyango et al., 2007), dolomite (Karaca et al., 2004) and fly ash (Ugurlu and Salman 1998) as well as some biomaterials including collagen fiber (Liao et al., 2006), shell powder (Namasivayam et al., 2005), banana stem (Anirudhan et al., 2006) and orange waste (Biswas et al., 2007) have been developed. Recently, the interest is focused on mesoporous materials, which have been applied for the removal harmful chemicals from water, such as arsenic, Hg, phenol (Yoshitake et al., 2003; Mangrulkar et al., 2008; Puanngam and Unob, 2008)

MCM-41, a mesoporous molecular sieve, has the characters of sharp and ordered pore distribution, high surface area and pore volume. Lanthanum is one of the rare earth elements that is considered to be pollution-free to environment and has an ability to adsorb phosphate. In the present article, Lanthanum doped meosoporous MCM-41(La_xM41) was prepared by sol-gel method. The effects of operating parameters on phosphate adsorption such as sorbent dosage, temperature, solution pH, contact time and initial phosphate concentration were evaluated. The fundamental adsorption behaviors of phosphate on La_{25}M41 from aqueous solutions were investigated, including the adsorption kinetics and adsorption isotherm.

1 Materials and methods

1.1 Reagents

All reagents were of analytical grade. Stock solutions of phosphate were prepared using anhydrous KH_2PO_4, and pH was pre-adjusted by HCl and NaOH solutions.

1.2 Synthesis of La_xM41

Lanthanum doped MCM-41 was synthesized by tetraethylorthosilicate as organic Si source and cetyltrimethylammonium bromide (CTAB) as template. The procedure is as follows: 9.6 g CTAB was added to

* Corresponding author. E-mail: zmshen@sjtu.edu.cn

the mixture of 160 g distilled water and 0.688 g NaOH; then 20 mL tetraethylorthosilicate was added slowly to the solution with stirring; after that, the lanthanum nitrate solution was introduced dropwise; the final mixture was stirred for 2 hr and then transferred into PTFE-lined autoclaves under autogenous pressure at 110°C for a period of 48 hr; the white solid produced was washed, filtered, dried, and calcined at 550°C with the heat rate of 1°C/min. The samples were presented as La_xM41, where x indicated the Si/La molar ratio (x = 100, 50, 25).

1.3 Characterization

X-ray powder diffraction patterns of the samples were recorded in the 2θ range of 0.8–8° with a scan speed of 1°/min using a diffractometer (D/max-2200/PC, Rigaku Corporation, Japan) with CuK_α radiation (40 mA, 45 kV). The pore structures distribution and BET area of the samples were measured at 77 K with N_2 physical adsorption/desorption technique using a surface area and porosimetry analyzer (ASAP 2010 M+C, Micromeritics Inc., USA). Prior to analysis, the La_xM41 was degassed at 200°C for 6 hr under vacuum (0.1 Pa). The La content of La_xM41 was determined by ICP (Iris Advantage 1000, Thermo Corporation, USA).

1.4 Phosphate adsorption

The adsorption capacity of La_xM41 toward phosphate was investigated using KH_2PO_4 solution. Adsorption experiments were carried out by batch experiments in 250 mL glass-stoppered conical flasks placed in an air bath thermostatic rotary shaker (HZQ-F, Harbin Donglian Electronic & Technology Development Co., Ltd, China). The sorbent (0.100 g) was mixed with 100 mL phosphate solution of various initial concentrations. The shake speed was kept constant at 120 r/min for all experiments. The supernatant solution was filtered by a 0.45-m syringe filter after the adsorption. The remaining phosphate concentration of the filtered solution was analyzed according to the ascorbic acid method of monitoring the absorbance at 880 nm on spectrophotometer (Unico UV-2102 PCS, Unico Corp., China) (APHA, 1985). The sorption amount of phosphate at equilibrium, q_e (mg/g), can be calculated by Eq. (1):

$$q_e = \frac{(C_0 - C_e)V}{m} \quad (1)$$

where, C_0 and C_e (mg/L) are the initial and equilibrium liquid phase phosphate concentrations, respectively, V (L) is the volume of the solution and m (g) is the mass of the dry sorbent used. All experiments were replicated twice and the mean values were reported.

2 Results and discussion

2.1 X-ray diffraction

The low-angle powder X-ray diffraction patterns of La_xM41 samples are depicted in Fig. 1. All samples exhibited well-resolved typical peaks of MCM-41 (100), (110), and (200), which is attributed to the *p6mm* mesoporous

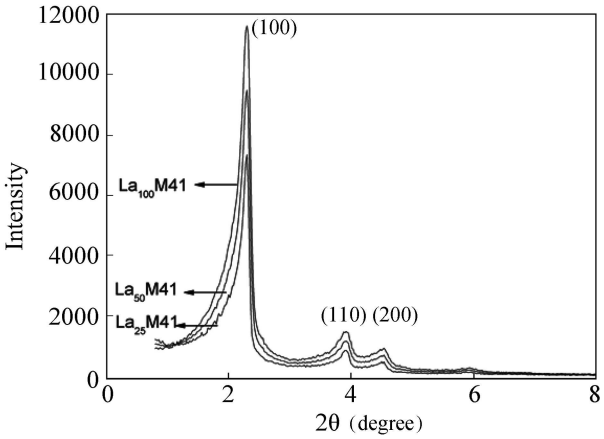

Fig. 1 X-ray diffraction patterns of $La_{100}M41$, $La_{50}M41$, and $La_{25}M41$.

structure. This indicated that moderate amount of La incorporated into MCM-41 did not change the hexagonal structure significantly. However, if a large amount of La incorporated the framework of doped MCM-41 would be disordered as reported by Qu et al. (2007)

2.2 N_2 adsorption/desorption isotherms

Nitrogen adsorption/desorption isotherms of all samples are shown in Fig. 2. All samples presented a typical reversible nitrogen adsorption/desorption isotherm of type IV, having an S-shape characteristic of MCM-41. The calculated BET surface areas and the mesoporous parameters are listed in Table 1. The BET surface areas of $La_{100}M41$, $La_{50}M41$, and $La_{25}M41$ were 914.3, 902.3, and 763.2 m^2/g, respectively. The corresponding pore sizes were 3.1, 3.4, and 3.6 nm. The incorporated La could cause a reduction of BET surface area, while the pore size increased with increasing of La introduced due to the

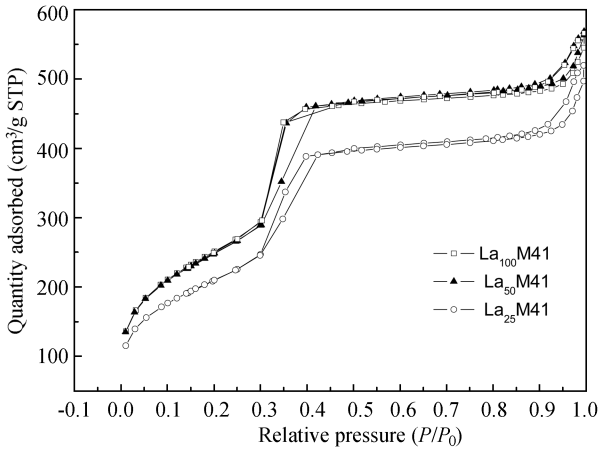

Fig. 2 Nitrogen adsorption/desorption isotherms of $La_{100}M41$, $La_{50}M41$, and $La_{25}M41$. STP: standard temperature pressure.

Table 1 Structure properties of La_xM41 determined by nitrogen adsorption/desorption

Sample	BET surface area (m^2/g)	Pore diameter (nm)	Total pore volume (cm^3/g)
$La_{100}M41$	914.3	3.1	0.88
$La_{50}M41$	902.3	3.4	0.88
$La_{25}M41$	763.2	3.6	0.80

substitution of silicon by La.

2.3 Effect of different Si/La molar ratio

Because MCM-41 did not adsorb phosphate, the phosphate adsorption is attributed to the La incorporation. For $La_{25}M41$, $La_{50}M41$, and $La_{100}M41$ the La contents were 7.53%, 3.89% and 2.32%, respectively. As shown in Fig. 3, with increasing amount of La, the phosphate adsorption capacity increased from 6.8 to 21.1 mg/g. The adsorption of the phosphate is usually characterized by either mass transfer or intraparticle diffusion or both for solid-liquid adsorption process. The mechanism of phosphate adsorption involves the chemical reaction between La on the adsorbents and phosphate forming metal-inorganic complexes. In term of the results, it was clearly that with the increase of La doped, the adsorption capacity of La_xM41 was significantly improved. Obviously, the key mechanism for phosphate removal was the precipitation of lanthanum phosphate formed by the reaction of doped lanthanum in La_xM41 with phosphate.

2.4 Effect of $La_{25}M41$ dose

Because $La_{25}M41$ has highest adsorption ability and relative fine mesoporous structure among studied absorbents, it was selected in the following experiment. Different doses of $La_{25}M41$ ranging from 0.100–0.500 g were added to 100 mL of a 50-mg/L phosphate solution for batch phosphate adsorption experiments. The effects of $La_{25}M41$ dose on the removal of phosphate and adsorption capacity are shown in Fig. 4. The phosphate removal increased with increasing $La_{25}M41$ dosage and reached the maximum 99.7% at 0.500 g, because a higher sorbent amount may provide a lager adsorbent surface area and more active sites. However, the adsorption capacity decreased from 21.15 to 9.97 mg/g with increasing amount of the sorbent from 0.100 to 0.500 g. The reason may be that increasing adsorbent dosage leads to an aggregation of adsorbent particles and increase in diffusion path length. Moreover, at constant phosphate concentration, the increase of adsorbent dosage will lead to an unsaturation of adsorption sites through the sorption process.

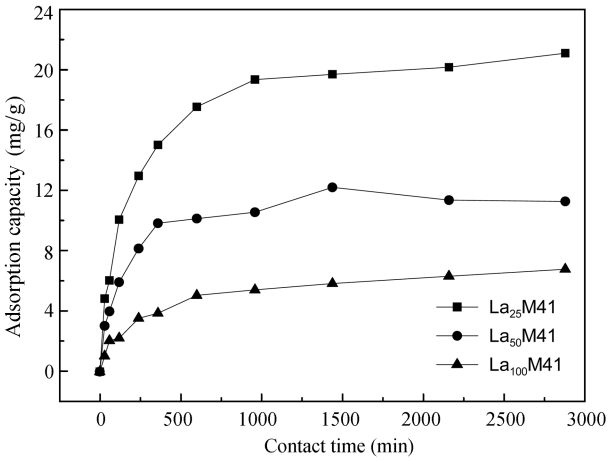

Fig. 3 Effect of different Si/La molar rations of La_xM41 on phosphate adsorption. Initial phosphate concentration: 50 mg/L; the amount of La_xM41: 0.100 g; pH: 7.0; the volume of solution: 100 mL; temperature: 25°C.

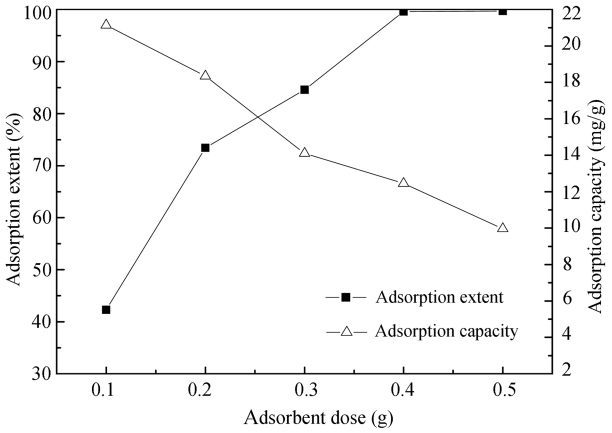

Fig. 4 Effect of the $La_{25}M41$ dose on removal extent and adsorption capacity of phosphate. Initial phosphate concentration: 50 mg/L; temperature: 25°C; stirring speed: 120 r/min; contact time: 1440 min.

2.5 Effect of initial pH

The solution pH can influence the adsorption of anions at the solid-liquid interface. This is partly because hydroxyl ions themselves intensively compete with adsorbate. The effect of pH on the adsorption of phosphate by $La_{25}M41$ was studied at pH range 2.0 to 12.0 (Fig. 5). The adsorption capacity of $La_{25}M41$ first increased with increase pH from 2.0 to 4.0 and reached a plateau with in pH from 4.0 to 8.0, then dramatically decreased to 8.0 mg/g at pH 12.0. This is because phosphate can exist in the form of H_3PO_4, $H_2PO_4^-$, HPO_4^{2-} and PO_4^{3-} which depend on the solution pH value. At pH ⩽ 3.0, predominant species of phosphate is H_3PO_4 which is weakly attached to the sites of the sorbent. With increase of solution pH, the dominant states transformed into $H_2PO_4^-$ and HPO_4^{2-}, which can be adsorbed by the sorbent. At pH 12.0, the OH^- concentration increased and competed with PO_4^{3-}. The electrostatic repulsion between the surface sites of highly negatively charged sorbent and anion do not favor the adsorption. In conclusion, neither low pH (pH ⩽ 4.0) nor high pH (pH > 8.0) was suitable for the adsorption.

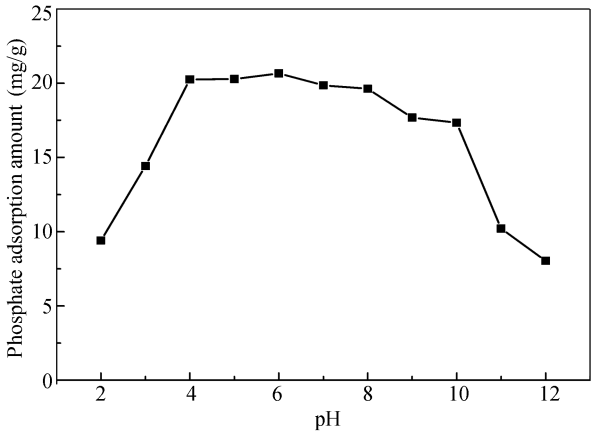

Fig. 5 Effect of pH on adsorption of phosphate. Adsorption dose: 0.1 g/100 mL; agitation time: 1440 min; temperature: 25°C.

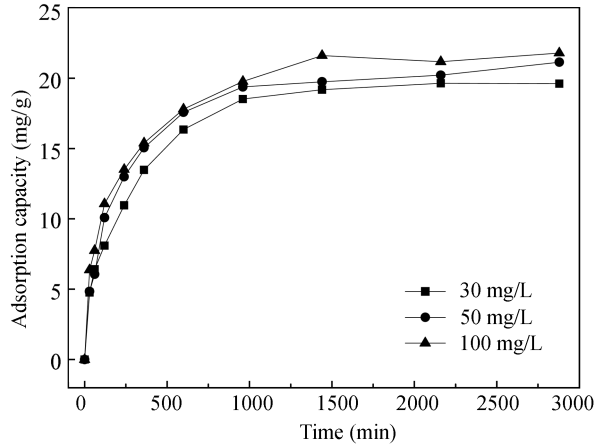

Fig. 6 Effect of agitation time and initial concentration on the amount of phosphate adsorbed onto $La_{25}M41$. Sorbent dosage: 100 mg/100 mL; pH: 7; temperature: 25°C; stirring speed; 120 r/min.

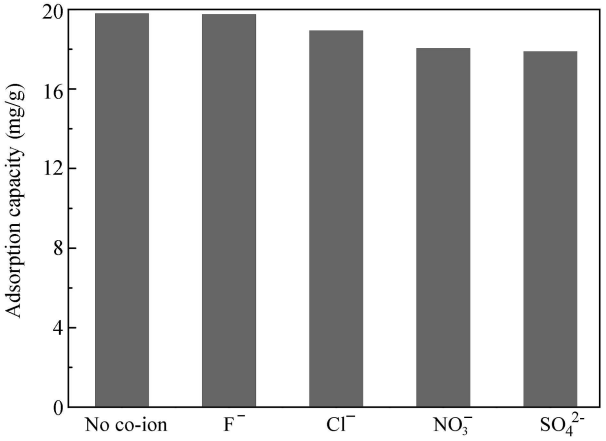

Fig. 7 Effect of foreign anions on adsorption capacity. Sorbent dosage: 0.100 g/100 mL; phosphate concentration: 50 mg/L; foreign anions concentrations: 400 mg/L; pH: 7; temperature: 25°C; stirring speed 120 r/min.

2.6 Effect of initial phosphate concentration and contact time

The effects of initial phosphate concentration and contact time on adsorption capacity are shown in Fig. 6. It is clear that adsorption capacity increased with the increase of initial phosphate concentration. The adsorption of phosphate increased with the lapse of time and reached to saturation after 960 min. The equilibrium time was independent of initial phosphate concentration. The maximum phosphate adsorption capacity was found to be 19.6, 21.1, and 21.8 mg/g at initial concentrations of 30, 50, and 100 mg/L at 25°C, respectively. However, the removal amounts of phosphate decreased from 65.3% to 22.2% with initial concentrations increasing from 30 to 100 mg/L. Because for a given sorbent dose, the total number of available active sites are fixed, while the relatively large number of active sites required for the high initial concentration of phosphate, the active sites are insufficient (Das et al., 2006). For $La_{25}M41$, the maximum adsorption capacity was calculate to be 22.0 mg/g, which is higher than the values reported previously (Li et al., 2009; Zeng et al., 2004)

2.7 Effect of co-existing anions

The effect of foreign anions on adsorption capacity were studied in the presence of sodium salts of following competing anions: F^-, Cl^-, NO_3^-, and SO_4^{2-} (Fig. 7). The results indicate that the addition of co-ions decreased the adsorption capacity of phosphate ions on $La_{25}M41$, due to the competition between the anions and phosphate for the adsorption sites on the adsorbent.

2.8 Adsorption kinetic studies

The pseudo first (Eq. (2)) and second-order (Eq. (3)) model were used to investigate the adsorption kinetic of phosphate onto the $La_{25}M41$ (Lagergren, 1898; Blanchard et al., 1984):

$$\log(q_e - q_t) = \log q_e - k_1 t/2.303 \quad (2)$$

$$\frac{t}{q_t} = \frac{1}{k_2 q_e^2} + \frac{t}{q_e} \quad (3)$$

where, q_e (mg/g) and q_t (mg/g) are the amount of phosphate adsorbed on sorbent at equilibrium and at time t (min), respectively. k_1 (min^{-1}) is the adsorption rate constant of pseudo first-order adsorption. The values of k_1 and q_e can be determined by the slope of linear plots of $\log(q_e - q_t)$ versus t. k_2 (g/(mg·min)) is the equilibrium rate constant of pseudo second-order adsorption. By plotting t/q versus t, values of k_2 and q_e can be calculated from the slope and intercept. According to the parameters obtained (Table 2) it can be concluded that pseudo second-order adsorption model was more suitable for describing the adsorption kinetics of phosphate on $La_{25}M41$.

2.9 Adsorption isotherm models

Langmuir and Freundlich isotherms were applied to describe the relationship between the amount of phosphate absorbed on $La_{25}M41$ and its equilibrium concentration in aqueous solution. The Langmuir isotherm, which is valid for monolayer adsorption onto surface with a finite number of identical sites, is expressed as Eq. (4):

$$\frac{C_e}{q_e} = \frac{1}{q_0 K_L} + \frac{C_e}{q_0} \quad (4)$$

Table 2 Comparison of the first and second-order adsorption rate constants and experimental values

Initial concentration (mg/L)	q_e (exp) (mg/g)	Pseudo first-order			Pseudo second-order		
		k_1 (min^{-1})	q_e (cal) (mg/g)	R^2	k_2 (g/(mg·min))	q_e (cal) (mg/g)	R^2
30	19.5	0.0023	16.3	0.966	0.000309	20.6	0.996
50	21.1	0.0025	16.8	0.976	0.000316	21.7	0.998
100	21.7	0.0028	16.9	0.994	0.000341	22.5	0.997

exp: experimental; cal: calculated.

Table 3 Langmuir and Freundlich isotherms constants

Temperature (°C)	Langmuir			Freundlich		
	Q (mg/g)	K_L (L/mg)	R^2	n	K_F (mg/g)	R^2
25	22.0	0.493	0.997	9.166	12.60	0.989
35	23.9	0.440	0.996	8.703	14.20	0.998
45	26.7	0.561	0.998	7.949	15.55	0.999

where, C_e (mg/L) is the concentration of phosphate solution at equilibrium, q_e (mg/g) is the amount of the phosphate absorbed by per unit of the sorbent, q_0 (mg/g) and K_L (L/mg) are Langmuir constants related to adsorption capacity and energy of adsorption, respectively.

The Freundlich isotherm is expressed as:

$$\log q_e = \log K_F + \frac{1}{n} \log C_e \quad (5)$$

where, K_F (mg/g) and n are the constants of the Freundlich isotherm that measure the adsorption capacity and intensity of adsorption, respectively.

The isotherm constants at 25, 35 and 45°C are summarized in Table 3. The equilibrium data obtained for the adsorption of phosphate on $La_{25}M41$ were fitted to Langmuir equation. The linear plots of C_e/q_e versus C_e at different temperatures were examined to determine q_0 and K_L values. The results indicate that the adsorption capacity increased from 22.0 to 26.7 mg/g as temperature increased. That may due to the increase of phosphate activity with the rising of temperature and easily diffusing to the mesoporous structure of the adsorbent. The extremely high values of the correlation coefficients confirm that both the Langmuir and Freundlich equations are suitable for describing the adsorption isotherm.

3 Conclusions

Lanthanum doped MCM-41 developed from sol-gel method is efficient for phosphate removal. Based on the results of X-ray diffraction, and N_2 adsorption/desorption, the structure of Lanthanum doped MCM-41 materials kept well, and La content in $La_{25}M41$, $La_{50}M41$, and $La_{100}M41$ was 7.53%, 3.89% and 2.32%, respectively. Phosphate adsorption matched with both Langmuir and Freundlich isotherms. Langmuir adsorption capacity was found to be 22.0 mg/g at 25°C. Kinetic data are described better by pseudo second-order model. The maximal adsorption was achieved with the pH range 3–8. Co-existing ions decreased the phosphate adsorption capacity. However, at present, the main problem is that the cost of La_xM41 preparation is high.

Acknowledgments

This work was supported by the National Major Research Plan for Water Pollution Control and Treatment of China (No. 2008ZX07101-015).

References

Anirudhan T S, Noeline B F, Mancihar D M, 2006. Phosphate removal from wastewaters using a weak anion exchanger prepared from a lignocellulosic residue. *Environmental Science & Technology*, 40(8): 2740–2745.

APHA (American Public Health Association), 1985. Standard Methods for the Examination of Water and Wastewater (16th ed.). Washington, DC, USA.

Biswas B K, Inoue K, Ghimire K N, Ohta S, Harada H, Ohto K et al., 2007. The adsorption of phosphate from an aquatic environment using metal-loaded orange waste. *Journal of Colloid and Interface Science*, 312(2): 214–223.

Blanchard G, Maunaye M, Martin G, 1984. Removal of heavy metals from waters by means of natural zeolites. *Water Research*, 18(12): 1501–1507.

Chubar N I, Kanibolotskyy V A, Strelko V V, Gallios G G, Samanidou V F, Shaposhnikova T O et al., 2005. Adsorption of phosphate ions on novel inorganic ion exchangers. *Colloids and Surfaces A: Physicochemical and Engineering Aspects*, 255(1-3): 55–63.

Das J, Patra B S, Baliarsingh N, Parida K M, 2006. Adsorption of phosphate by layered double hydroxides in aqueous solutions. *Applied Clay Science*, 32(3-4): 252–260.

Georgantas D A, Grigoropoulou H P, 2007. Orthophosphate and metaphosphate ion removal from aqueous solution using alum and aluminum hydroxide. *Journal of Colloid and Interface Science*, 315(1): 70–79.

Karaca S, Gurses A, Ejder M, Acikyildiz M, 2004. Kinetic modeling of liquid-phase adsorption of phosphate on dolomite. *Journal of Colloid and Interface Science*, 277(2): 257–263.

Li H, Ru J, Yin W, Liu X H, Wang J Q, Zhang W D, 2009. Removal of phosphate from polluted water by lanthanum doped vesuvianite. *Journal of Hazardous Materials*, 168(1): 326–330

Liao X P, Ding Y, Wang B, Shi B, 2006. Adsorption behavior of phosphate on metal-ions-loaded collagen fiber. *Industrial and Engineering Chemistry Research*, 45(11): 3896–3901.

Mangrulkar P A, Kamble S P, Meshram J, Rayalu S S, 2008. Adsorption of phenol and *o*-chlorophenol by mesoporous MCM-41. *Journal of Hazardous Materials*, 160(2-3): 414–421.

Namasivayam C, Sakoda A, Suzuki M, 2005. Removal of phosphate by adsorption onto oyster shell powder – kinetic studies. *Journal of Chemical Technology & Biotechnology*, 80(3): 356–358.

Onyango M S, Kuchar D, Kubota M, Matsuda H, 2007. Adsorptive removal of phosphate ions from aqueous solution using synthetic zeolite. *Industrial and Engineering Chemistry Research*, 46(3): 894–900.

Ou E, Junjie Z J, Shaochun M C, Jiaqiang W Q, Fei X, Liang M, 2007. Highly efficient removal of phosphate by lanthanum-doped mesoporous SiO_2. *Colloids and Surfaces A: Physicochemical and Engineering Aspects*, 308(1-3): 47–53.

Puanngam M, Unob F, 2008. Preparation and use of chemically modified MCM-41 and silica gel as selective adsorbents for Hg(II) ions. *Journal of Hazardous Materials*, 154(1-3): 578–587.

Lagergren S, 1898. Zur theorie der sogenannten adsorption gelöster stoffe. Kungliga Svenska Vetenskapsakademiens, *Handlingar*, 24(4): 1–39.

Saad R, Belkacemi K, Hamoudi S, 2007. Adsorption of phosphate and nitrate anions on ammonium-functionalized MCM-48: Effects of experimental conditions. *Journal of Hazardous Materials*, 311(2): 375–381.

Ugurlu A, Salman B, 1998. Phosphorus removal by fly ash. *Environment International*, 24(8): 911–918.

Yoshitake H, Yokoi T, Tatsumi T, 2003. Adsorption behavior of arsenate at transition metal cations captured by amino-functionalized mesoporous silicas. *Chemistry of Materials*, 15(8): 1713–1721.

Zeng L, Li X M, Liu J D, 2004. Adsorptive removal of phosphate from aqueous solutions using iron oxide tailings. *Water Research*, 38(5): 1318–1326.